Transition frequencies in the (2-0) band of D2 with MHz accuracy

Didier Mondelain, S. Kassi, Alain Campargue

Transition frequencies in the (2-0) band of D_2 with MHz accuracy

D. Mondelain*, S. Kassi, A. Campargue

Univ. Grenoble Alpes, CNRS, LIPhy, 38000 Grenoble, France

*Corresponding author: Didier Mondelain (didier.mondelain@univ-grenoble-alpes.fr)

Key words

Deuterium; hydrogen; D2; transition frequencies; CRDS; frequency comb

Abstract

Series of spectra of the *S*(0) and *Q*(1)-*Q*(4) transitions of the (2-0) band of D_2 near 5860 cm^{-1} are recorded by comb-referenced cavity ring down spectroscopy at four pressures up to 200 Torr. After averaging, high resolution (30 MHz step) and low noise (noise equivalent absorption, $\alpha_{min} \approx 1.5\times10^{-11}$ cm^{-1}) spectra are obtained for each pressure value. This leads to signal to noise ratios of several hundred for the considered very weak electric quadrupole transitions with intensities ranging between 4×10^{-29} and 4×10^{-28} cm/molecule. The *Q*(3) and *Q*(4) transitions are newly detected.

A multi-spectrum treatment of the D_2 line profiles at different pressures performed using a quadratic speed-dependent Nelkin-Ghatak profile leads to residuals close to the noise level. Considering statistical fit errors and possible biases, total uncertainties on the frequencies extrapolated at zero pressure are estimated between 0.30 MHz and 1.83 MHz. The derived experimental frequencies and intensities of (2-0) transitions are gathered with literature values and compared to *ab initio* values reported in *J. Komasa, M. Puchalski, P. Czachorowski, G. Łach, K. Pachucki, Phys. Rev. A 100, 032519 (2019)*. An agreement within the combined uncertainties is achieved for the *S*(0), *Q*(1), *Q*(2) and *Q*(3) transitions. Line intensities are also discussed in relation with literature values.

1. Introduction

The hydrogen molecule (H_2) and its isotopologues (HD, D_2) are the most simple neutral molecular systems, allowing thus for sophisticated *ab initio* calculations of their electronic ground state rovibrational energies [1,2,3]. Very recently, updated calculations have been made available including relativistic and quantum electrodynamic (QED) corrections and leading to accuracy on the transition frequencies between 10^{-3} and 10^{-7} cm^{-1} [4]. The accuracy achieved in the calculations of the hydrogen spectrum gives an exceptional opportunity for a constructive interplay between theory and experiment. This matter of fact motivated recent experimental efforts to determine the absolute frequency of different absorption and Raman transitions for H_2 [5,6,7,8,9,10,11], HD [5,12,13,14,15] and D_2 [5,16,17,18,19,20,21,22,23]. Transition frequencies reported with an accuracy down to a 10^{-9} relative uncertainty provide crucial tests of quantum electrodynamic theory and interesting insights for physics beyond the Standard Model [24].

In the case of the symmetric species (H_2, D_2), the absorption spectrum consists of weak electric quadrupole (E2) vibrational bands. In the case of the HD isotopologue, the isotopic substitution leads to the appearance of a small electric dipole and the HD spectrum includes both electric dipole (E1) and E2 transitions. As a result, the HD spectrum is dominated by E1 bands which provide the most stringent tests for *ab initio* calculations. In particular, the accuracy of the line centre determination in HD transitions has been considerably improved in Ref. [13] and Ref. [14] using saturation spectroscopy. Accuracies of 80 kHz and 20 kHz have been reported for the frequency of the *R*(1) transition in the (2-0) overtone band, respectively. Nevertheless, the two values show a difference of ~1 MHz, largely beyond their combined accuracies even if the latter uncertainty was recently reconsidered and increased to 50 kHz because of a complex hyperfine structure [15].

In the case of D_2, the intensity of the E2 lines are several orders of magnitude weaker and saturation spectroscopy is hardly achievable. An accurate determination of the line centre in Doppler regime requires thus both a very high sensitivity and a high accuracy of the frequency axis. Highly sensitive techniques, such as CRDS, allow recordings at low pressures, minimizing the error due to extrapolation of the measured positions to zero pressure which is required for comparison to theory. Nowadays, the accurate calibration of the frequency axis of the recorded spectra can be achieved by linking the experimental setup to an optical frequency comb (OFC) referenced to an atomic clock [25]. This method has been recently applied to the determination of the *S*(2) transition frequency of the (2-0) band of D_2 [21,22] near 6204 cm^{-1} in Doppler regime. Line centers reported with small uncertainties of

500 kHz and 390 kHz, respectively, show a difference of 540 kHz, thus within the combined error bars. These experimental values were in disagreement with the best *ab initio* value provided at that time with a difference (~4 MHz) close to the 3σ uncertainty on the calculated value [22]. Nevertheless, the latest calculations [4] show a better agreement (1 MHz difference instead of 4 MHz [22]) with these combined experimental values and a reduced uncertainty (0.75 MHz [4] instead of 1.25 MHz [22]). The Torun group has recently re-measured the same transition with an improved accuracy of 160 kHz with a frequency-stabilized cavity ring-down spectrometer in the frequency agile, rapid scanning spectroscopy (FARS) mode [26]. This most recent value shows a larger difference of 1590 kHz (~5.3×10^{-5} cm^{-1}) compared to the theoretical value of Ref. [4] reported with a 1σ uncertainty of 750 kHz.

The aim of the present contribution is to measure frequencies of other transitions of the same (2-0) band of D_2 with an accuracy at the MHz level or below in order to provide further validation tests of the latest *ab initio* calculations available [4]. An overview of the (2-0) band as predicted by *ab initio* calculations is presented in **Fig. 1**. If we except the first observation of the *Q*(1)-*Q*(3) lines at high pressure (>35 bar) [27], previous absorption studies of (2-0) transitions are limited to *(i)* the *S*(0)-*S*(3) transitions reported by Gupta et al. by off-axis ICOS with position uncertainties between 3 MHz and 300 MHz retrieved from a standard Voigt profile analysis, [16] *(ii)* our previous CRDS study of the *Q*(1), *Q*(2) and *S*(0)-*S*(8) transitions including the extremely weak *S*(8) line among the weakest absorption lines ever reported (line intensity of 1.8×10^{-31} cm/molecule), which were analyzed using a Galatry line profile [20] and *(iii)* the above mentioned studies dedicated to the high accuracy determination of the *S*(2) line center [21,22,26].

In the present work, the *Q*(1)-*Q*(4) and the *S*(0) absorption lines are measured (see **Fig. 1**). The very weak *Q*(3) and *Q*(4) lines are detected for the first time. The positions of the *S*(0), *Q*(1) and *Q*(2) transitions were previously reported by CRDS in [20] with an accuracy limited to 30 MHz due to the absence of an absolute reference standard to calibrate the frequency axis. In the present experiment, an important gain on the frequency accuracy is achieved by linking the CRDS setup to a frequency comb referenced to a GPS referenced 10 MHz rubidium clock. In the following, the setup and spectra recordings are described (Part 2). Then, the data analysis, line profile fitting procedures together with the evaluation of the uncertainties on the measured transition frequencies will be presented in Part 3 before comparison to *ab initio* calculations (Part 4).

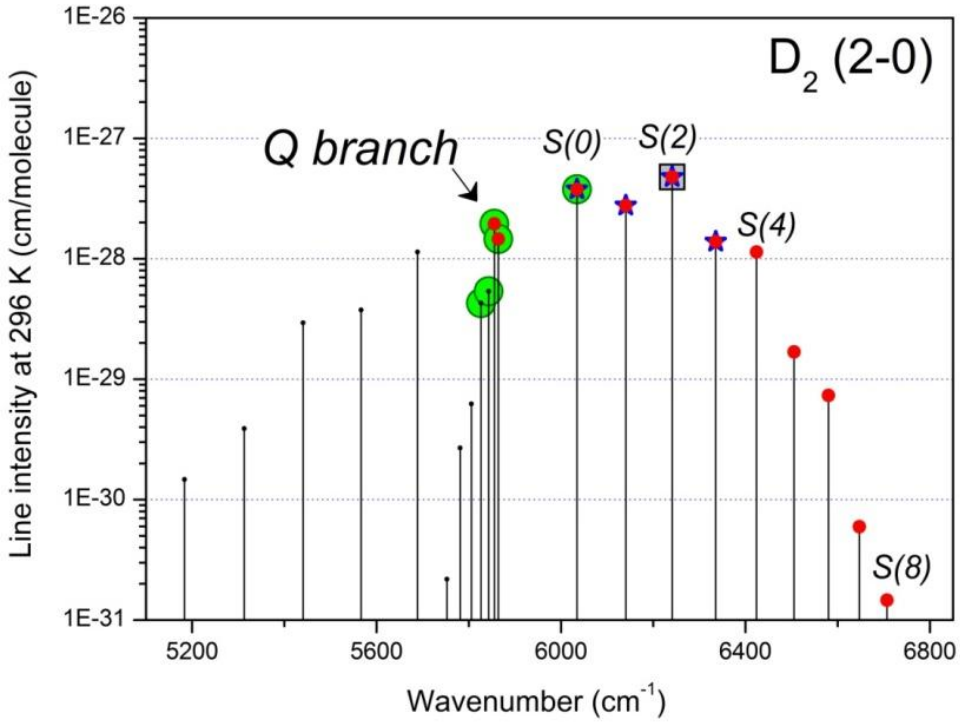

Figure 1. *Overview of the calculated spectrum of the (2-0) band of D_2 [16]. The lines studied in Ref. [16], Ref. [20] and in this work are marked with red dots, blue stars and green circles, respectively. The S(2) transition (square) was studied in Refs [21,22] and very recently in [26].*

2. Experimental setup and spectra recordings

The frequency comb referenced CRDS method and setup used for the recordings have been described in details in Refs. [28,29]. The accurate frequency values associated "on the fly" to each ring-down value allows not only for an absolute calibration of the frequency axis but also for a more accurate characterization of the line profile due to a reduced noise amplitude in particular on the sharp slopes of the line profile [30,31,32].

Here, four distributed feedback (DFB) laser diodes were employed to measure the *S*(0), *Q*(1)-*Q*(4) transitions. The optical cavity was fitted with two high reflectivity mirrors optimized between 5435 cm^{-1} and 5780 cm^{-1} leading to finesse between 130 000 for the *Q*(4) transition around 5826 cm^{-1} and 50 000 for the *S*(0) transition around 6035 cm^{-1}. Typical beat note widths of 700 kHz at the 1 ms time scale were measured between the different laser diodes and a tooth of a self-referenced frequency comb (from Menlo Systems). This provides the absolute frequency of the laser light, f_{exp}, for each ring down (RD) event from:

$$f_{exp} = f_{DFB} + f_{AOM} = f_{CEO} + nf_{rep} \pm f_{BN} + f_{AOM} \qquad \text{Eq. (1)}$$

The 250 MHz repetition rate, f_{rep}, and the carrier-envelop offset, f_{CEO}, (here equal to -20 MHz) of the comb were referenced to a GPS referenced 10 MHz rubidium clock. The beat

note frequency, f_{BN}, was determined at a 1 kHz repetition rate by Fourier transforming, with a 7 kHz resolution, the photodiode signal digitalized with a fast ADC (250 MHz sampling rate). The frequency of the sinusoidal wave, f_{AOM}, applied to the acousto-optic modulator, used to obtain the RD events by switching off the laser light in the cavity, was delivered by a direct digital synthesizer (DDS). Both the fast ADC clock and DDS were referenced to the 10 MHz reference.

Series of spectra for pure D_2 (Aldrich, chemical purity of 99.999% with atomic deuterium isotopic abundance of 99.96%) were recorded in static regime for each transition at four different pressures between 50 and 200 Torr (see **Table 1**). For a single scan, the noise equivalent absorption (NEA) evaluated as the *rms* of the baseline fluctuations varies between 6.5×10^{-11} and 8×10^{-11} cm^{-1} for the $Q(1)$-$Q(4)$ transitions and is around 2×10^{-10} cm^{-1} for the $S(0)$ transition because of the much shorter RD time of ~80 µs instead of ~200 µs at lower wavenumbers. The gas pressure in the optical cavity was continuously monitored using a 1000 mbar pressure gauge (Model 622 Barocel pressure sensor from Edwards, 0.15% accuracy of the reading) and the temperature of the cell was measured with a temperature sensor (TSic 501, IST-AG, ±0.1 K accuracy) fixed on the cell surface, covered by an external blanket for thermal isolation. During all the recordings the mean temperature was 295 K with an excursion of ±0.5 K.

Transition	$S(0)$	$Q(1)$	$Q(2)$	$Q(3)$	$Q(4)$
Pressure. (Torr)	75/100/150/200	50/75/100/150	50/75/100/150	50/75/100/150	75/100/125/150
Nb of spectra	27/28/16/14	26/19/29/14	33/33/24/19	37/27/28/18	45/23/28/17

***Table 1**. Recording pressures and corresponding number of spectra acquired for each absorption line of the (2-0) band of D_2.*

The number of spectra (between 14 and 45) recorded for each transition and each pressure value is included in **Table 1** leading to a total of more than 500 spectra with a typical duration of 10 min each. Each spectrum (typically 0.3 cm^{-1} to 0.5 cm^{-1} wide) is composed of several ten thousands of RD events, each of them associated to an absolute frequency calculated from Eq. (1). In order to reduce the amount of data, an averaging procedure was applied to each series of spectra corresponding to a given pressure value. It consists in gathering the CRDS measurement points within 30 MHz wide bins, removing the outliers, and averaging. As a result, typical NEA of 1.5×10^{-11} cm^{-1} was achieved after averaging.

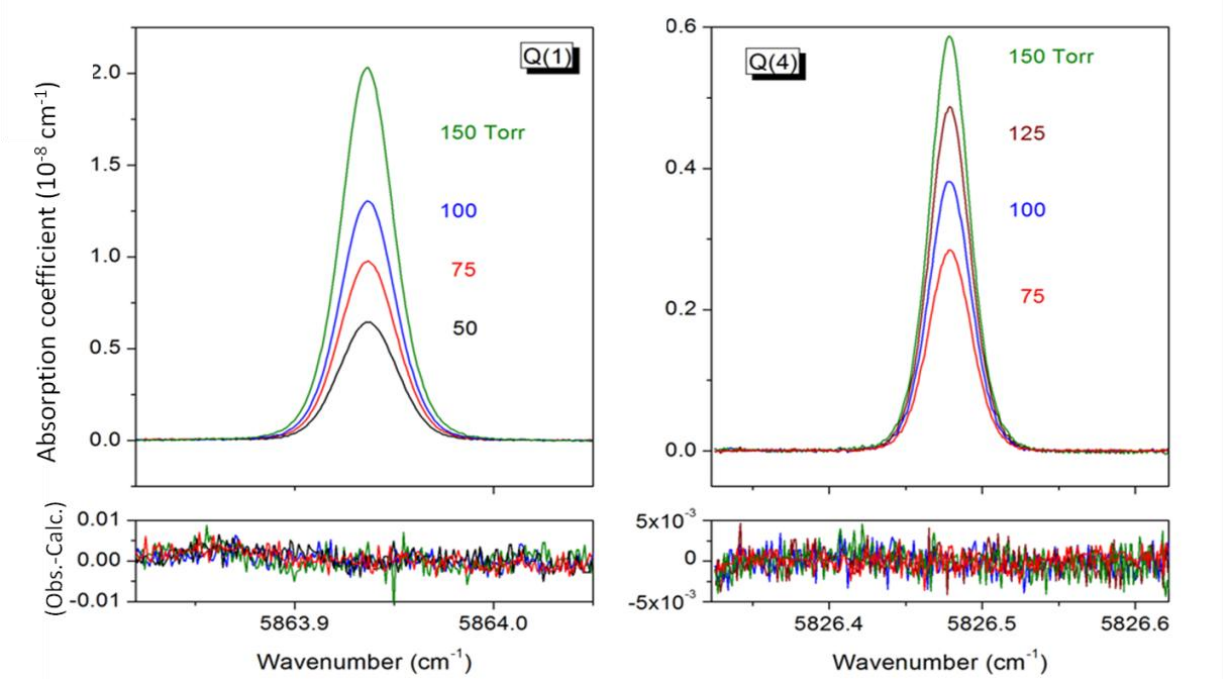

***Figure 2**. Averaged spectra of the Q(1) (left panel) and Q(4) (right panel) transitions in the first overtone band of D_2, at four pressure values. The lower panels show the residuals obtained from a multi-spectrum treatment using a qSDNG profile (see Text). Note the different scale between the left- and right-hand panels.*

Figure 2 shows the pressure dependence of the averaged line profile of the *Q*(1) and *Q*(4) lines. Signal to noise ratios between 280 and 580 are achieved for the *Q*(4) line despite maximum absorption coefficients of few 10^{-9} cm^{-1}. For the *Q*(1) line, it reaches a value of more than 1000 for the highest pressure.

3. Data analysis and uncertainty budget

The first step of the spectra analysis was to remove the contribution of some weak impurity lines overlapping with the D_2 lines of interest. As a result of the high sensitivity of the recordings, lines due water vapor and methane present with relative abundance of ~10 ppm and a few tens ppb, respectively, were observed in the spectra. For each averaged spectrum, corresponding to a given pressure value, the contribution of these interfering species was simulated with the HITRAN2016 database [33] and a Voigt profile and then subtracted (see **Figure 3**).

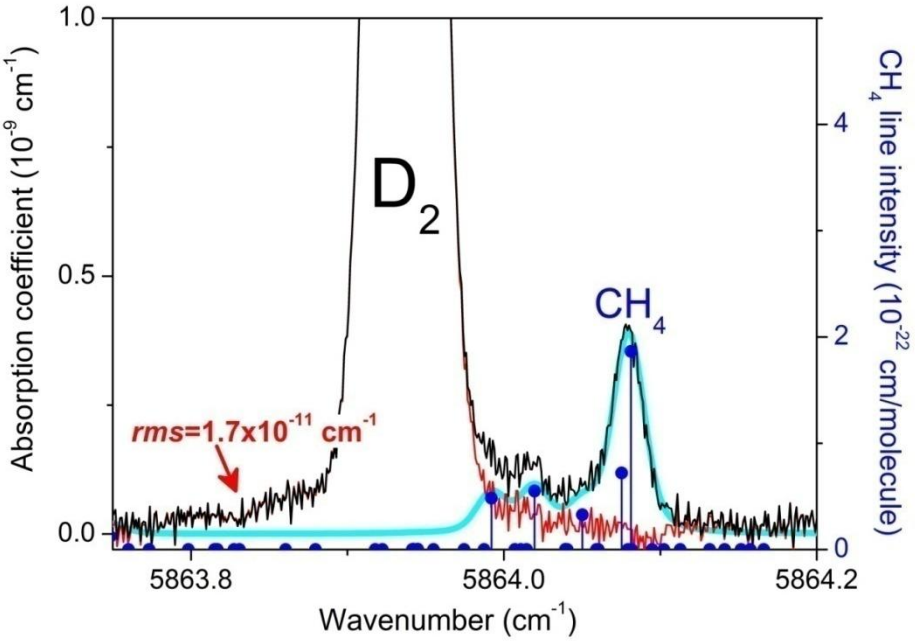

Figure 3*. Spectrum of the (2-0) Q(1) transition of D_2 recorded at 50 Torr after averaging (black line) and subtracting the contribution of methane present as an impurity with a few tens ppb relative concentration (red line). The CH_4 transitions provided by the HITRAN2016 database (blue circles) and the simulated methane spectrum (cyan solid line) are also shown.*

The averaged spectra free of impurity lines were used for a line profile fit of the D_2 transitions. As illustrated in **Figure 4**, the standard Voigt profile is not sufficient to account for the observation. Dicke effect, characterized by the frequency of the velocity-changing collisions parameter, ν_{VC}, in the hard-collision model, and speed dependence of the broadening and shift (γ_2 and δ_2, respectively), modeled with a quadratic law here, lead to the narrowing and asymmetry of the line profile. A home-made multi-spectrum fitting program was used to fit the parameters of the quadratic speed-dependence Nelkin-Ghatak (qSDNG) profile [34,35,36,37]. For each spectrum, the baseline (including the contribution of the collision induced absorption (CIA) [38]) was assumed to be a quadratic polynomial of the wavenumber and adjusted by the fit. The multi-spectrum fitting procedure constrained the pressure broadening coefficient (γ_0) and the ν_{VC}, γ_2, δ_2 parameters to be identical for the different pressure values but the positions and line areas were fitted independently for each spectrum, δ_0, being fixed to zero. **Figure 2** shows the quality of the profile reproduction for the $Q(1)$ and $Q(4)$ transitions using a qSDNG profile. The residuals of the fit displayed on the lower panel of **Fig. 2** are close to the noise level (1.8×10^{-11} cm^{-1} and 1.3×10^{-11} cm^{-1} for $Q(1)$ and $Q(4)$, respectively). The derived line parameters are listed in **Table 2.**

The position at zero pressure, ν_0 and the pressure shift coefficient were retrieved from a weighted linear fit of the fitted positions *versus* the pressure. Each data point was weighted

according to the inverse of its squared uncertainty (evaluated below). Similarly, the line intensity, *S(T)*, was obtained from the proportionality factor of the areas *versus* the pressure.

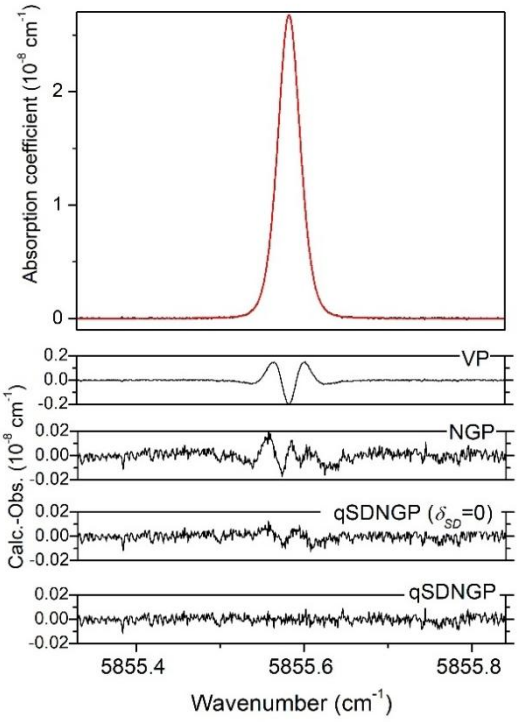

Figure 4*. Averaged spectrum of the Q(2) transition at 150 Torr (upper panel). The residuals obtained after subtraction of the spectrum fitted with Voigt (VP), Nelkin-Ghatak (NGP) and quadratic speed-dependent Nelkin-Ghatak (qSDNGP) profiles are shown on the lower panels. Note the ×10 scaling between the residuals for the Voigt profile and for the other profiles.*

An inaccurate determination of the spectrum baseline or of the concentration of the interfering species contributes to the error budget of the position (and intensity). To evaluate this possible bias, we fitted each averaged spectrum alone because each spectrum can be affected differently. Hence, we investigated the influence of a change by ±25% of the CH_4 and H_2O concentrations, this variation corresponding to a mismatch of the concentration clearly visible in the residuals. Similarly, we estimated the impact of the baseline by varying the spectral range over which the fit was performed. These type-B uncertainties [39] were used to weight the positions and areas in the above described fit of the zero-pressure positions, line intensities and self-pressure shift parameters. The obtained fitted values of ν_0, *S(296 K)* and δ_0 are included in **Table 2** with their corresponding statistical uncertainty provided by the fit. The final uncertainty on the transition frequency range between 0.30 MHz and 1.83 MHz. Note that the signal-to-noise ratio of our spectra allowed us to evidence and take into account the asymmetry of the line shape which has an impact on the obtained line center.

Table 2. *Line shape parameters obtained from multi-spectrum treatment of the CRDS spectra recorded for a series of pressure values. The δ_0, γ_0, ν_{VC}, γ_2,* and *δ_2 values are given in $10^{-3}cm^{-1}atm^{-1}$ Unit. For a pressure series, the γ_0, ν_{VC}, γ_2,* and *δ_2 values were constrained to be identical but the line centers and line areas were fitted independently for each spectrum, and used afterwards to derive the zero-pressure position (ν_0,), line intensity, S(T) and self- pressure shift (δ_0). Line intensities were converted to the usual reference temperature (296 K).*

Transition	ν_0 (cm^{-1})	*S(296 K)* *(10^{-28} cm/molecule)*	δ_0	γ_0	ν_{VC}	γ_2	δ_2
***Q*(4)**	5826.479104(37)	0.423(8)	-2.03(6)	4.32	10.97	6.81	0.53
***Q*(3)**	5843.084584(61)	0.525(12)	-2.43(32)	5.74	8.62	8.27	0.28
***Q*(2)**	5855.583358(14)	1.930(20)	-2.47(8)	5.45	10.52	6.70	0.69
***Q*(1)**	5863.937052(29)	1.463(49)	-2.43(17)	7.83	6.44	10.18	0.52
***S*(0)**	6034.650463(10)	3.692(31)	-2.11(5)	3.96	11.76	5.76	0.69

The δ_0, γ_0, ν_{VC}, γ_2, and δ_2 parameter values are plotted on **Figure 5** *versus m*, where *m= J"* and *J"+1* for the *Q* and *S* branch, respectively. A clear numerical correlation between γ_0, ν_{VC} and γ_2 parameters is observed γ_0 and γ_2 evolving similarly with *m* while ν_{VC} is anticorrelated to these parameters (see discussion in Ref. [22]).

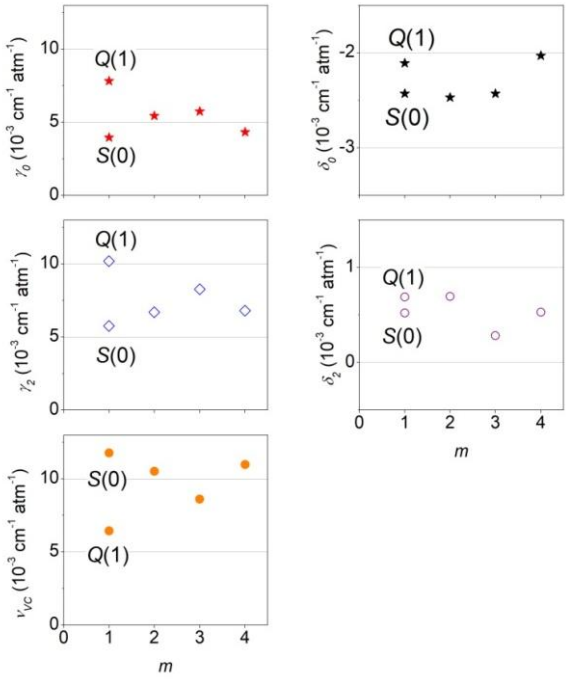

Figure 5. *Overview of the line profile parameters of the S(0) and Q(1)-Q(4) transitions of the (2-0) band of D_2 versus m where m=J" and J"+1 for the Q and S branch, respectively.*

4. Comparison with *ab initio* calculations

In **Table 3**, we have gathered the positions and intensities and their final uncertainties, obtained in this work with literature values relative to the (2-0) band of D_2 [16,20,21,22,26]. The table includes the *ab initio* position values and uncertainties provided by the computer code of Ref. [40] supported by calculations of Ref. [4]. The experimental and theoretical

uncertainties and the difference between the experimental and calculated values are plotted in **Figure 6**. For the *S*(0) and *Q*(1)-*Q*(4) transitions studied here, the uncertainty on the calculated values is about 2×10^{-5} cm^{-1}, on the same order than the experimental error bars ranging between 1.0×10^{-5} cm^{-1} and 6.2×10^{-5} cm^{-1}. The agreement between the calculated and measured positions is satisfactory with maximum differences of 1.5 times the combined uncertainties.

Our previous CRDS determination of the *Q*(1)-*Q*(2) and *S*(0)-*S*(8) line centers [16] was reported with uncertainties larger than 10^{-3} cm^{-1} (30 MHz) because the frequency calibration at that time relied on some water reference line center known with such accuracy. These previous measured frequencies show a reasonable agreement with *ab initio* values within the experimental error bar. This is not the case for the *S*(2) position value measured by the off-axis ICOS technique which show deviations of more than 6×10^{-4} cm^{-1} while it was reported with an claimed error bar of 10^{-4} cm^{-1} (**Figure 6**).

The *S*(2) line center is the one which was determined with the highest accuracy both in our group [21] (510 kHz) and in the Torun's group [22] (390 kHz). An agreement within the error bars is observed between the newly reported *ab initio* value (6241.127614(25) cm^{-1}) [4,40] and the combined experimental value (6241.127647(11) cm^{-1}) derived from measurements of Refs. [21,22]. The line center of this transition has recently been re-measured with an improved accuracy of 160 kHz with a frequency-stabilized CRDS in the FARS mode leading to a value of 6241.1276670(54) cm^{-1} [26]. This value shows a difference of 1590 kHz (~5.3×10^{-5} cm^{-1}) with the theoretical value *i. e.* 2.1 times the combined uncertainties.

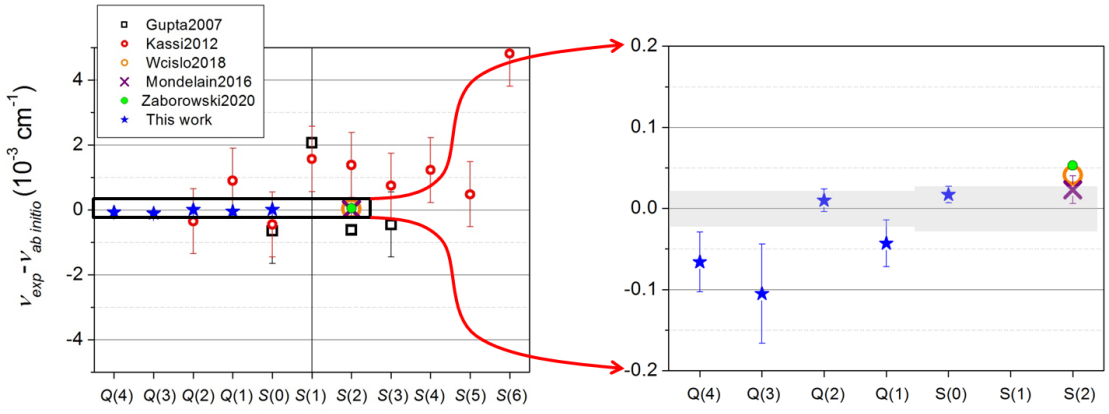

Figure 6. Differences between the wavenumbers obtained experimentally for the Q(1)-Q(4) and S(0)-S(6) transitions [16,20,21,22,26] and the calculated values from computer code [40] supported by calculations of Ref. [4]. The grey rectangles on the right panel represent the theoretical uncertainties [40]. All the error bars are given at 1σ.

The difference between the J= 0 and J= 2 ground state levels can be obtained using combination difference relations of the $Q(2)$ and $S(0)$ experimental and *ab initio* [4] wavenumbers of these transitions. An excellent agreement (~5×10^{-6} cm^{-1} or 150 kHz) is obtained between the calculated and measured values as reflected by the very close (exp.- *ab initio*) deviations of the $Q(2)$ and $S(0)$ transitions plotted in **Figure 6** (to be compared to an absolute uncertainty on the calculated ground state energy levels around 1.5×10^{-4} cm^{-1} [4,40]).

Only three sources of experimental intensities are available for comparison with *ab initio* calculations (**Table 3** and **Figure 7**). The intensities measured in this work with error bars ranging between 0.8 and 3.3% show differences of a few percent compared to the calculated values reported with relative uncertainties below 0.1% [16]. The largest difference concerns the $S(0)$ transition for which a deviation close to 3σ is observed while the previous determination of Ref. [16] was much closer to the *ab initio* value. For the $Q(1)$, $Q(2)$ and $S(0)$ transitions, our intensity values agree with the previous CRDS values [16] within the error bars. Again, the error bars reported by Gupta et al. [20] seem largely underestimated. Deviations of +20.8 and -8.8 % are noticed for the $S(0)$ and $S(0)$ intensities reported with uncertainties of only 0.45% and 0.3%, respectively, which seems unrealistic considering the simple Voigt profile used in that reference. We note that overall our present intensity values have the tendency to be smaller than calculated values but the differences remain close to the experimental error bars. Unfortunately, the Torun group limited their study of the $S(2)$ line to a sophisticated profile analysis and did not report the corresponding intensity value which would have been particularly valuable for comparison.

Pressure-shift coefficients given in Refs. [16,20] are included in **Table 3** for comparison purpose. Note that the listed δ_0 values relative to our work differ from those given in **Table 2**: as most of the literature values did not consider an asymmetric profile in their analysis, we performed a new multi-spectrum analysis constraining δ_2 to be zero. An agreement within 1σ is observed with [16] for the $S(0)$ and $Q(1)$ transitions but a discrepancy larger than 3σ is noticed for the $Q(2)$ transition. A large disagreement with [20] is also observed for the $S(0)$ transition.

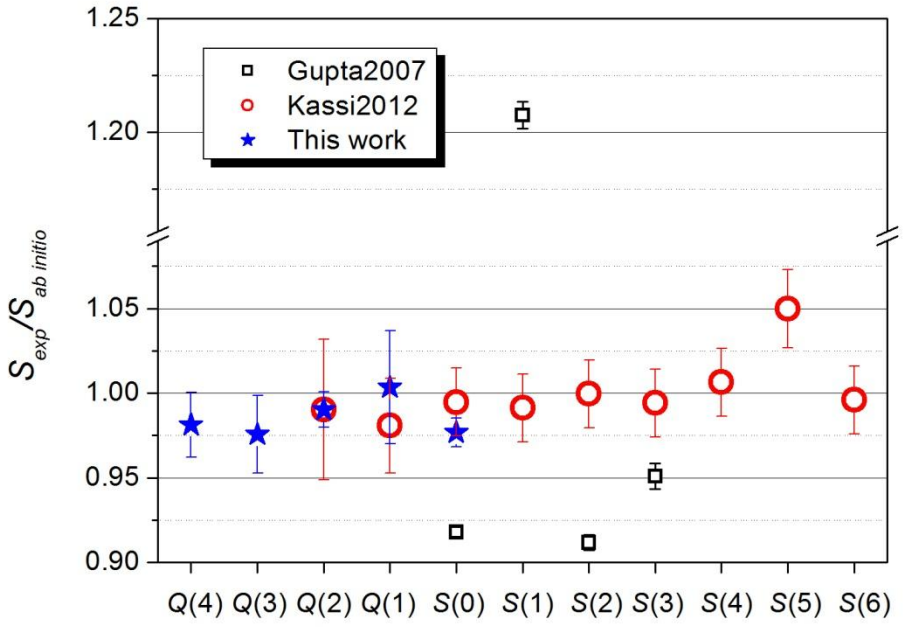

Figure 7. Ratios between the intensities obtained in this work and in Refs [16,20] for the Q(1)-Q(4) and S(0)-S(6) transitions and the calculated values [16]. All the error bars are given at 1σ. Note the break on the y-axis scale.

5. Conclusion

Thanks to series of spectra recorded at different pressures using a CRDS spectrometer linked to a rubidium clock referenced frequency comb, accurate transition wavenumbers were determined for the very weak *Q*(1)-*Q*(4) and *S*(0) transitions for the (2-0) band of D_2. (line intensities between 4×10^{-29} cm/molecule and 3.7×10^{-28} cm/molecule). Accuracies between 330 kHz and 1860 kHz have been achieved corresponding to relative uncertainties from 1.8×10^{-9} to 1.0×10^{-8}. Two of these very weak transitions, *Q*(4) and *Q*(3), are measured for the first time. Comparison with the latest *ab initio* frequencies [4, 40] shows a good agreement within the combined uncertainties for *S*(0), *Q*(1), *Q*(2) and *Q*(3) transitions confirming the validity of the high order QED corrections of the calculations.

Table 3. Centre, intensity and pressure shift coefficient for the transitions of the (2-0) band of D_2. Comparison with calculated values.

Trans.	Line position			Line intensity at 296 K			Reference [c]
	Calc. (cm^{-1}) [40]	Meas. (cm^{-1})	δ_0 [a] (10^{-3} cm^{-1} atm^{-1})	Calc. [16] (10^{-28} cm/molecule)	Meas. (10^{-28} cm/molecule)	Relative Difference(%) [b]	
Q(4)	5826.479170(22)	**5826.479104(37)**	**-2.53(20)**	**0.428**	**0.420(8)**	**-1.9(19)**	**This work**
Q(3)	5843.084689(22)	**5843.084584(61)**	**-2.54(34)**	**0.537**	**0.524(12)**	**-2.4(23)**	**This work**
Q(2)	5855.583348(22)	5855.583(1)	-2.16(18)	1.949	1.93(8)	-1.0(40)	Kassi2012
		5855.583358(14)	**-2.99(8)**		**1.930(20)**	**-1.0(10)**	**This work**
Q(1)	5863.937095(22)	5863.938(1)	-2.67(12)	1.458	1.43(4)	-1.9(28)	Kassi2012
		5863.937052(29)	**-2.85(18)**		**1.463(49)**	**+0.3(33)**	**This work**
S(0)	6034.650446(24)	6034.650(1)	-2.33(25)	3.780	3.76(7)	-0.5(20)	Kassi2012
		6034.6498(10)	-2.169(26)		3.47(1)	-8.2(3)	Gupta2007
		6034.650463(10)	**-2.63(6)**		**3.692(31)**	**-2.3(8)**	**This work**
S(1)	6140.618429(24)	6140.620 (1)	−1.7(4)	2.774	2.75(6)	+0.8(20)	Kassi2012
		6140.6205(100)	−1.978(92)		3.35(2)	+20.8(6)	Gupta2007
S(2)	6241.127614(25)	6241.129 (1)	−2.5(5)	4.782	4.78(9)	-0.0(20)	Kassi2012
		6241.1270(1)	−1.536(28)		4.36(2)	-8.8(5)	Gupta2007
		6241.127637(17)					Mondelain2016
		6241.127655(13)	[a]				Wcislo2018
		6241.127667(5)	[a]				Zaborowski2020
S(3)	6335.717250(25)	6335.718 (1)		1.388	1.38(3)	+0.6(20)	Kassi2012
		6335.7168(10)	−1.805(22)		1.32(1)	+4.9(8)	Gupta2007
S(4)	6423.966767(26)	6423.968 (1)	−1.859(76)	1.138	1.145(22)	+0.6(20)	Kassi2012
S(5)	6505.501516(26)	6505.502 (1)	−1.8(5)	0.1686	0.177(4)	+5.0(23)	Kassi2012
S(6)	6579.997182(27)	6580.002 (1)	−2.6	0.07349	0.0732	+0.4(20)	Kassi2012

Notes

[a] Literature values of δ_0 obtained with asymmetric line profiles are not reported in this table. The δ_0 values of our measurements differ from those listed in **Table 2**. For comparison purpose, they have been obtained with δ_2 fixed to zero (see Text).

[b] (Meas.-Calc.)/Calc.×100

[c] Previous works: Gupta2007 [20], Kassi2012 [16], Mondelain2016 [21], Wcislo2018 [22] and Zaborowski2020 [26].

References

[1] Pachucki K, Komasa J. Nonadiabatic corrections to rovibrational levels of H_2. J Chem Phys 2009;130:164113. doi :10.1063/1.3114680

[2] Piszczatowski K, Lach G, Przybytek M, Komasa J, Pachucki K, Jeziorski B. Theoretical Determination of the Dissociation Energy of Molecular Hydrogen. J Chem Theory Comput 2009;5:3039-3048. Doi: 10.1021/ct900391p

[3] Komasa J, Piszczatowski K, Łach G, Przybytek M, Jeziorski B, Pachucki K, Quantum Electrodynamics Effects in Rovibrational Spectra of Molecular Hydrogen. J Chem Theory Comput 2011;7:3105-3115. Doi:10.1021/ct200438t

[4] Komasa J, Puchalski M, Czachorowski P, Łach G, Pachucki K, Rovibrational energy levels of the hydrogen molecule through nonadiabatic perturbation theory. Phys Rev A 2019;100:032519. Doi: 10.1103/PhysRevA.100.032519

[5] Dickenson GD, Niu ML, Salumbides EJ, Komasa J, Eikema KSE, Pachucki K, Ubachs W. Fundamental Vibration of Molecular Hydrogen. Phys Rev Lett 2013;110: 193601. Doi: 10.1103/PhysRevLett.110.193601

[6] Salumbides EJ, Dickenson GD, Ivanov TI, Ubachs W. QED Effects in Molecules: Test on Rotational Quantum States of H_2. Phys Rev Lett 2011;107:043005. Doi: 10.1103/PhysRevLett.107.043005

[7] Campargue A, Kassi S, Pachucki K, Komasa J. The absorption spectrum of H_2: CRDS measurements of the (2-0) band, review of the literature data and accurate ab initio line list up to 35 000 cm^{-1}. Phys Chem Chem Phys. 2012;14:802-815. Doi: 10.1039/C1CP22912E

[8] Kassi S, Campargue A. Electric quadrupole transitions and collision-induced absorption in the region of the first overtone band of H_2 near 1.25 μm. J Mol Spectrosc 2014; 300:55. Doi: 10.1016/j.jms.2014.03.022

[9] Cheng CF, Sun YR, Pan H, Wang J, Liu AW, Campargue A, Hu SM. Electric-quadrupole transition of H_2 determined to 10^{-9} precision. Phys Rev A 2012;85:024501. Doi: 10.1103/PhysRevA.85.024501

[10] Tan Y, Wang J, Cheng CF, Zhao XQ, Liu AW, Hu SM. Cavity ring-down spectroscopy of the electric quadrupole transitions of H_2 in the 784–852 nm region. J Mol Spectrosc 2014;300:60-64. Doi: 10.1016/j.jms.2014.03.01

[11] Niu ML, Salumbides EJ, Ubachs W. Test of quantum chemistry in vibrationally hot hydrogen molecules. J Chem Phys 2015;143:081102. Doi: 10.1063/1.4929568

[12] Kassi S, Campargue A. Electric quadrupole and dipole transitions of the first overtone band of HD by CRDS between 1.45 and 1.33 μm. J Mol Spectrosc 2011;267:36-42. Doi : 10.1016/j.jms.2011.02.001.

[13] Tao LG, Liu AW, Pachucki K, Komasa J, Sun YR, Wang J, Hu SM. Toward a determination of the proton-electron mass ratio from the lamb-dip measurement
of HD. Phys Rev Lett 2018;120:153001. Doi: 10.1103/PhysRevLett.120.153001

[14] Cozijn FMJ, Dupré P, Salumbides EJ, Eikema KSE, Ubachs W. Sub-doppler frequency metrology in hd for tests of fundamental physics. Phys Rev Lett 2018;120:153002. Doi: 10.1103/PhysRevLett.120.153002

[15] Diouf ML, Cozijn FMJ, Darquié B, Salumbides EJ, Ubachs W. Lamb-dips and lamb-peaks in the saturation spectrum of HD. Opt Lett 2019;44:4733–4736. Doi: 10.1364/OL.44.004733

[16] Kassi S, Campargue A, Pachucki K, Komasa J. The absorption spectrum of D_2: Ultrasensitive cavity ring down spectroscopy of the (2–0) band near 1.7 μm and accurate ab initio line list up to 24 000 cm^{-1}. J Chem Phys 2012;136:184309. Doi : 10.1063/1.4707708

[17] Maddaloni P, Malara P, De Tommasi E, De Rosa M, Ricciardi I, Gagliardi G, Tamassia F, Di Lonardo G, De Natale P. Absolute measurement of the S(0) and S(1) lines in the electric quadrupole fundamental band of D_2 around 3 μm. J Chem Phys 2010;133:154317. Doi: 10.1063/1.3493393

[18] Fakhr-Eslam SH, Sheldon GD, Sinclair PM, Drummond JR, May AD. Anomalous broadening and shifting in D_2 and D_2–He mixtures. J Quant Spectrosc Radiat Transf 2001;68:377-399. Doi: 10.1016/S0022-4073(00)00031-5

[19] Borysow J, Fink M. NIR Raman spectrometer for monitoring protonation reactions in gaseous hydrogen. J Nucl Mater 2005;341;224-230. Doi: 10.1016/j.jnucmat.2005.02.002

[20] Gupta M, Owano T, Baer DS, O'Keefe A. Quantitative determination of the (2,0) band of deuterium in the near infrared via off-axis ICOS. Chem Phys Lett 2007;441: 204-208. Doi: 10.1016/j.cplett.2007.05.031

[21] Mondelain D, Kassi S, Sala T, Romanini D, Gatti D, Campargue A. Sub-MHz accuracy measurement of the S(2) 2–0 transition frequency of D_2 by Comb-Assisted Cavity Ring Down spectroscopy. J Mol Spectrosc 2016;326:5–8. Doi: 10.1016/j.jms.2016.02.008

[22] Wcisło P, Thibault F, Zaborowski M, Wójtewicz S, Cygan A, Kowzan G, Masłowski P, Komasa J, Puchalski M, Pachucki K, Ciuryło R, Lisak D. Accurate deuterium spectroscopy for fundamental studies. J Quant Spectrosc Radiat Transf 2018;213:41–51. Doi: 10.1016/j.jqsrt.2018.04.011

[23] Martínez, RZ, Bermejo, D, Wcisło, P, Thibault, F. Accurate wavenumber measurements for the $S_0(0)$, $S_0(1)$, and $S_0(2)$ pure rotational Raman lines of D_2. J Raman Spectrosc. 2019; 50: 127– 129. Doi:10.1002/jrs.5499

[24] Ubachs W, Koelemeij JCJ, Eikema KSE, Salumbides EJ. Physics beyond the Standard Model from hydrogen spectroscopy. J Molec Spectrosc 2016;320:1–12. Doi: 10.1016/j.jms.2015.12.003
[25] Margolis HS. Spectroscopic applications of femtosecond optical frequency combs. Chem Soc Rev 2012;41:5174–5184. Doi: 10.1039/c2cs35163c
[26] Zaborowski M, Słowinski M, Stankiewicz K, Thibault F, Cygan A, Józwiak H, Kowzan G, Masłowski P, Nishiyama A, Stolarczyk N, Wójtewicz S, Ciuryło R, Lisak D, Wcisło P. Ultra-high finesse cavity-enhanced spectroscopy for accurate tests of quantum electrodynamics for molecules. arXiv:2001.10979 [physics.atom-ph]
[27] Brannon PJ, Church CH, Peters CW. Electric field induced spectra of molecular hydrogen, deuterium and deuterium hydride. J Mol Spectrosc 1968;27:44-54. Doi: 10.1016/0022-2852(68)90018-0
[28] Mondelain D, Kassi S, Sala T, Romanini D, Marangoni M, Campargue A. Sub-MHz accuracy measurement of the S(2) 2–0 transition frequency of D_2 by comb-assisted cavity ring down spectroscopy J Mol Spectrosc 2016;326:5-8. doi:10.1016/j.jms.2016.02.008
[29] Mondelain D, Mikhailenko SN, Karlovets EV, Béguier S, Kassi S, Campargue A. Comb-Assisted Cavity Ring Down Spectroscopy of ^{17}O enriched waterbetween 7443 and 7921 cm^{-1}. J Quant Spectrosc Radiat Transf 2017;203:206-12. 10.1016/j.jqsrt.2017.03.029
[30] Tran DD, Tran H, Vasilchenko S, Kassi S, Campargue A, Mondelain D. High sensitivity spectroscopy of the O_2 band at 1.27 μm: (II) air-broadened line profile parameters. J Quant Spectrosc Radiat Transf 2020;240:106673. Doi: 10.1016/j.jqsrt.2019.106673
[31] Konefał M, Kassi S, Mondelain D, Campargue A. High sensitivity spectroscopy of the O_2 band at 1.27 μm: (I) pure O_2 line parameters above 7920 cm^{-1}. J Quant Spectrosc Radiat Transf 2020;241:106653. Doi: 10.1016/j.jqsrt.2019.106653
[32] Vasilchenko S, Tran H, Mondelain D, Kassi S, Campargue A. Accurate absorption spectroscopy of water vapor near 1.64 μm in support of the MEthane Remote LIdar missioN (MERLIN). J Quant Spectrosc Radiat Transf 2019;235:332–342. Doi: 10.1016/j.jqsrt.2019.06.027
[33] Gordon IE, Rothman LS, Hill C, Kochanov RV, Tan Y, Bernath PF, Birk M, Boudon V, Campargue A, Chance KV, Drouin BJ, Flaud JM, Gamache RR, Hodges JT, Jacquemart D, Perevalov, VI, Perrin A, Shine KP, Smith MAH, Tennyson J, Toon GC, Tran H, Tyuterev VG, Barbe A, Császár, AG, Devi VM, Furtenbacher T, Harrison JJ, Hartmann J-M, Jolly A, Johnson TJ, Karman T, Kleiner, I, Kyuberis AA, Loos J, Lyulin OM, Massie ST, Mikhailenko SN, Moazzen-Ahmadi N, Müller HSP, Naumenko OV, Nikitin AV, Polyansky OL, Rey M, Rotger M, Sharpe SW, Sung K, Starikova E, Tashkun SA, Vander Auwera J, Wagner G, Wilzewski J, Wcisło P, Yu S, Zak EJ. The HITRAN2016 Molecular Spectroscopic Database. J Quant Spectrosc Radiat Transf 2017;203:3-69. doi: 10.1016/j.jqsrt.2017.06.038
[34] Ngo NH, Lisak D, Tran H, Hartmann J-M. An isolated line-shape model to go beyond the Voigt profile in spectroscopic databases and radiative transfer codes. J Quant Spectrosc Radiat Transf 2013;129:89–100. Doi : 10.1016/j.jqsrt.2013.05.034
[35] Tran H, Ngo NH, Hartmann J-M. Efficient computation of some speed-dependent isolated line profiles. J Quant Spectrosc Radiat Transf 2013;129:199–203. Doi: 10.1016/j.jqsrt.2013.06.015
[36] Ngo NH, Lisak D, Tran H, Hartmann J-M . Erratum to “An isolated line-shape model to go beyond the Voigt profile in spectroscopic databases and radiative transfer codes” [J. Quant. Spectrosc. Radiat. Transf. 129 (2013) 89–100]. J Quant Spectrosc Radiat Transf 2014;134:105.
[37] Tran H, Ngo NH. Hartmann J-M Erratum to "Efficient computation of some speed-dependent isolated line profiles" [J Quant Spectrosc Radiat Transfer 129 (2013) 199-203]. J Quant Spectrosc Radiat Transf 2014;134:104.
[38] Frommhold, L. Collision-Induced Absorption in Gases (Cambridge Univ. Press, Cambridge, 1994).
[39] Evaluation of measurement data - Guide to the expression of uncertainty in measurement, JCGM 100:2008.
[40] H2SPECTRE ver. 7.0 Fortran source code, 2019, https://www.fuw.edu.pl/~krp/codes.html; http://qcg.home.amu.edu.pl/qcg/public_html/H2Spectre.html; P. Czachorowski, Ph.D. thesis, University of Warsaw, Poland, 2019.